OPINION

Turing's next steps: the mechanochemical basis of morphogenesis

Jonathon Howard, Stephan W. Grill and Justin S. Bois

Abstract | Nearly 60 years ago, Alan Turing showed theoretically how two chemical species, termed morphogens, diffusing and reacting with each other can generate spatial patterns. Diffusion plays a crucial part in transporting chemical signals through space to establish the length scale of the pattern. When coupled to chemical reactions, mechanical processes — forces and flows generated by motor proteins — can also define length scales and provide a mechanochemical basis for morphogenesis.

In his seminal paper "The chemical basis of morphogenesis", published in 1952, Alan Turing described a thought experiment in which he suggested "that a system of chemical substances, called morphogens, reacting together and diffusing through a tissue, is adequate to account for the main phenomena of morphogenesis" (REF. 1). By morphogenesis, Turing was thinking of the spatial patterning of biological tissues — patterns like the arrangements of the spots on a leopard's skin or a butterfly's wing, or the periodicities of the stripes on a seashell or a fish's body. In the paper, Turing gave a specific example of a reaction–diffusion mechanism in which a slowly diffusing, 'local' activator and a rapidly diffusing 'long-range' inhibitor, through their mutual interactions, reached steady-state concentrations that varied with position with a well-defined spatial period[2]. He argued that such molecules could be responsible for the patterning of biological tissues.

The morphogen has become a central concept in developmental biology[3]. Since the discovery of the first morphogen, the transcription factor Bicoid (BCD) in the *Drosophila melanogaster* zygote[4], small diffusing molecules have been shown to act as morphogens that control cell fate decisions in *Dictyostelium discoideum* (for example, cyclic AMP) and in vertebrate development (for example, retinoic acid). Spatial patterns of these morphogens have a length scale that defines the size of the features of the pattern. Turing's insight was that diffusion, with reaction, can specify length scales. Since he originally proposed his theory, reaction–diffusion mechanisms have been central to our thinking about pattern formation during development (see REF. 5 for a recent review).

> "Turing also realized the importance of mechanics — stress, motion and elasticity — in morphogenesis"

Interestingly, Turing also realized the importance of mechanics — stress, motion and elasticity — in morphogenesis, even though he did not know about the molecular basis of biological force generation: the sliding-filament mechanism of muscle contraction was not elucidated until a few years after the morphogenesis paper[6,7], and dynein and kinesin were not discovered until the 1960s and 1980s, respectively[8–10]. Turing defined the state of a system undergoing morphogenesis as consisting of "two parts, the mechanical and the chemical", and explicitly stated that both parts should be taken into account. Because "the interdependence of the chemical and mechanical data adds enormously to the difficulty," he "proposed to give attention rather to cases where the mechanical aspects can be ignored and the chemical aspects are most significant," although he did suggest that this difficulty might be circumvented with "the aid of a digital computer."

Indeed, it has become clear that active mechanical processes, such as transport along cytoskeletal filaments, cytoplasmic flow and endocytosis, also have essential roles in patterning at the cell and tissue levels. These processes provide mechanisms beyond simple diffusion for transporting signals through space. In this Opinion article, we discuss how active transport and mechanical forces, when coupled to chemical reactions, can define the length scales associated with patterning in cells and tissues.

Patterning processes and their speeds

Chemical reactions are inherently local phenomena, so they cannot form spatial patterns alone; a non-local process must also be at work for the patterning of biochemical species. Turing proposed that thermal diffusion (also known as Brownian motion), which is the process by which chemical species are distributed randomly by thermal forces, provides the long-range process that is required for patterning. The distance travelled by thermal diffusion is proportional to $\sqrt{(Dt)}$, in which D is the diffusion coefficient and t is time, and diffusive transport is fast over short distances, but slow over long ones. A much-debated question is whether thermal diffusion is fast enough to account for the spatial patterns that can be observed in cells and tissues[11]. The answer, of course, depends on the speed of development: if development is slow enough that morphogens cover the required distances by diffusive transport, thermal diffusion suffices. However, if development is too fast, other processes that are faster than thermal diffusion, such as active motor-driven processes, may be necessary and can dominate over diffusive ones in pattern formation.

There are two prominent mechanical processes that act faster (over long distances) than thermal diffusion, and both require an energy source. First, there is directed transport driven by motor proteins, a type of advection. The speed (v) of a typical motor protein is about 1 μm s^{-1} (REF. 12). By contrast, the diffusion coefficient of a typical protein undergoing Brownian motion is about 5 μm^2 s^{-1} (REF. 13); it will diffuse ≈3 μm in 1 s. Beyond a distance defined by D/v (≈5 μm for a typical protein), motor-driven transport overtakes diffusion[14]. Thus, in eukaryotic cells, the diameters of which are typically greater than 10 μm, advection will usually outpace thermal diffusion. This is especially true for larger protein complexes and vesicles, the diffusive motion of which can be greatly slowed down by obstructions, such as cytoskeletal filaments and other cytoplasmic structures[13].

A useful way to compare the relative importance of directed, advective transport to diffusion is via the Péclet number, which is defined as the ratio of the diffusion time to the advection time ($Pe = vL/D$, in which L is the relevant distance): if the Péclet number is much less than 1 (short distances), diffusion dominates; if the Péclet number is much greater than 1 (long distances), advective transport dominates. In large cells, such as oocytes or cells in plant stems, the flow of cytoplasm, owing to motility of motor proteins at the cell periphery (cytoplasmic streaming), results in a large Péclet number[15,16], indicating that advection dominates over diffusion. In multicellular tissues, active transport through the individual cells, as well as circulation of extracellular fluids driven by muscle or ciliated cells[17], is also expected to dominate over thermal diffusion.

Motor-driven transport can also result in active diffusion, which is so named to distinguish it from thermal diffusion. If cargoes randomly switch between motors of opposite directionality, or motors randomly switch between filaments of opposite orientation (such as the microtubules in dendrites[18]), then the long-time motion is undirected overall. Active diffusion can also be characterized by a diffusion coefficient (the value of which is $\sim v^2 \Delta t$, in which v is the motor speed and Δt is the switching time). This active diffusion coefficient is often, but not always, larger than the thermal diffusion coefficient. For example, 0.5-μm-diameter pigment globules in *Xenopus laevis* skin cells are transported by myosin V motors on a randomly oriented actin network with an active diffusion coefficient of ≈0.1 μm^2 s^{-1} (REF. 19), orders of magnitude greater than would be expected for thermal diffusion of a particle of that size[13]. Similarly, in the *D. melanogaster* oocyte, particles containing mRNA and protein move back and forth driven by Kinesin-1 moving along microtubules of nearly random orientation: the slight bias of microtubule orientation leads to a slow posterior drift that is superimposed on a random motion with diffusion coefficient ≥0.5 μm^2 s^{-1} (REF. 20). For small particles, such as single proteins, it is difficult to determine whether the random motion of molecules observed in cells is driven by active processes or by thermal forces. In the case of an inert molecule, such as green fluorescent protein (GFP), diffusion in cytoplasm is probably driven by thermal forces; in the case of phagosomes in *D. discoideum* cells, force measurements indicate that diffusion is driven by active processes[21].

A second process that acts faster than diffusion is movement due to mechanical stress. Forces exerted by motor proteins on the cytoskeleton can travel extremely quickly through cells and tissues, at the speed of sound in the material. Even for very soft tissues, such as the brain[22], the speed of sound is ≈1 m s^{-1}, which is a million times faster than diffusion and motor-driven transport. Active or elastic stress differences lead to rapid movement of material in many contexts, such as in flows of the actin cortex in a developing embryo[23,24] or growth of pollen tubes[25]. Morphogens embedded in these materials are moved along with them, and this is another example of advection. Furthermore, mechanical stress can influence chemical processes by pulling motor proteins off their filaments[26] or by unfolding proteins to reveal cryptic binding sites[27]. Therefore, long-range mechanical stress can generate biochemical patterns with length scales exceeding those that can be generated by diffusion alone.

Mechanochemical length scales

In his original paper, Turing stated that mechanical stresses and motions, diffusion and chemical reactions should all be taken into account when studying pattern formation. However, because of the mathematical difficulties associated with treating mechanochemical coupling, he developed a detailed theory only for coupling of chemical reactions with diffusion. In this section, we first review the special case of reaction–diffusion pattern formation mechanisms. Then we describe patterns resulting from coupling of chemical reactions with motor transport and mechanical stresses, the more general mechanochemical basis for morphogenesis. The focus throughout is to understand the physical principles that lead to the emergence of the length-scales of the patterns.

Patterns generated by local source–global sink mechanisms. In the case of a reaction–diffusion process in which a molecule is created at one end of a cell or tissue,

Glossary

Active diffusion
Random motion caused by randomly directed active forces, such as those generated by motor proteins.

Advection
Directed transport driven by motor proteins or bulk fluid flow.

Diffusion
The randomly directed motion of a molecule or particle that causes both mixing and the flux of particles from regions of high concentration to low concentration. Diffusion can be caused by thermal forces — that is, collisions with molecules in solution — or by randomly directed active forces, such as those generated by motor proteins that randomly change their direction.

Diffusion coefficient
The constant of proportionality between the flux and the concentration gradient for a diffusing particle. Diffusion can be thermal or active.

Friction coefficient
The constant or proportionality between a stress gradient and velocity.

Length constant
The distance over which a quantity such as concentration decreases e-fold.

Morphogens
Substances, such as proteins or small molecules, that are non-uniformly distributed in space and can influence cell growth or differentiation.

Patterning
The establishment of features that are much larger than those of the individual molecular components, and which are stereotyped from one cell to another or one organism to another.

Reaction–diffusion mechanism
A patterning process in which a diffusing morphogen undergoing chemical reactions (such as degradation or synthesis) forms a well-defined spatial distribution.

Stress
Force per unit area.

Viscoelastic material
A material that is both elastic (it can be stretched but returns to its original shape) and viscous (it deforms at a finite speed determined by the viscosity and the applied stress).

Viscosity
The constant of proportionality between rates of stress and strain (the relative deformation of a solid body due to a stress).

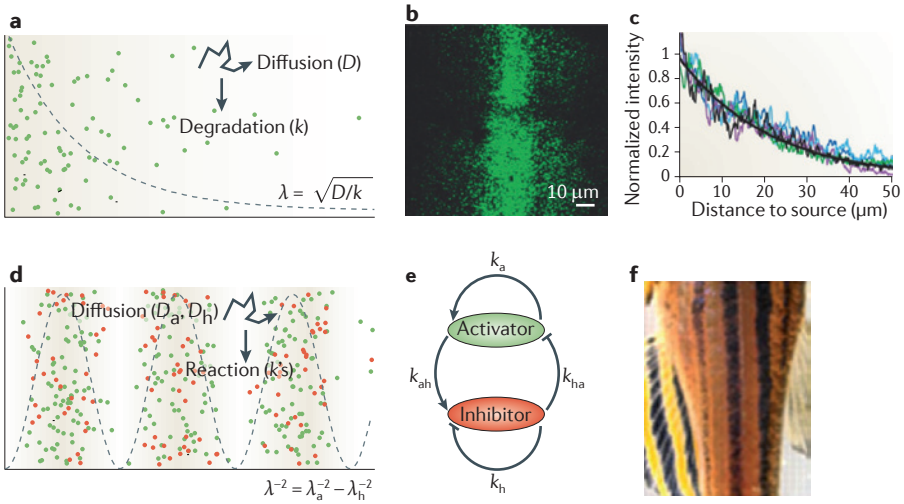

Figure 1 | **Patterning of biochemical species by reaction–diffusion mechanisms. a** | Schematic of a local source–global sink mechanism. Morphogens (green dots) are released at a point and degrade as they diffuse away. The steady-state concentration of the molecule decreases exponentially, with a length constant given by $\lambda = \sqrt{(D/k)}$, in which D is the diffusion coefficient and k is the rate constant of degradation. **b**,**c** | Green fluorescent protein (GFP)-tagged Decapentaplegic (DPP) patterning in a developing fly wing (**b**). DPP diffuses away from the source, the vertical line along which the intensity is highest, and is degraded in the tissue to give an exponential gradient[32] (**c**). **d**,**e** | Schematic of a 'Turing pattern' (**d**) featuring two chemical species (activator shown in green and inhibitor in red), with the reaction scheme in **e**. As a result of self-amplification, a peak in activator and inhibitor concentration grows. Because the inhibitor diffuses away from a peak more quickly than the activator, it has higher concentrations relative to the activator on either side of the peak, thereby restricting the width to which the peak may spread. The distance between the peaks in the pattern, λ, is a complicated function of the diffusion coefficients and rate constants defined in **e**. At the onset of pattern formation, λ is given by the formula shown in **d**, in which $\lambda_a = \sqrt{(D_a/k_a)}$ and $\lambda_h = \sqrt{(D_h/k_h)}$; 'a' represents the activator and 'h' represents the inhibitor. **f** | The stripes on a zebrafish are thought to be generated by a Turing mechanism[41]. Images in parts **b** and **c** are modified, with permission, from REF. 32 © (2007) The American Association for the Advancement of Science. Image in part **f** is reproduced, with permission, from REF. 41 © (2009) National Academy of Sciences.

diffuses away and is degraded over time, the steady-state concentration of the molecule decreases exponentially with a length constant given by $\lambda = \sqrt{(D/k)}$, in which k is the rate of degradation[28,29] (FIG. 1a). The length constant in this case is the average distance the molecule moves before it is degraded.

There are several examples of reaction–diffusion gradients. One is the gradient of activity of the small GTPase Ran, which regulates the assembly of the mitotic spindle[30,31]. The source of active Ran is chromatin, where a guanine nucleotide exchange factor catalyses the conversion of inactive RanGDP into active RanGTP. The global sink is the cytoplasm, where a soluble Ran GTPase-activating protein converts RanGTP back into the inactive GDP-bound form. The length constant is ≈5 μm, and the localized activity of Ran restricts the desequestration of spindle assembly factors to the immediate vicinity of the spindle.

Another example of a reaction–diffusion source–sink process is the gradient of the morphogen Decapentaplegic (DPP), which controls growth and patterning in the developing fly wing[32] (FIG. 1b). The gradient forms by a combination of randomly directed movement away from a source and degradation in the tissue; the length constant is ≈20 μm (FIG. 1c). Although the diffusion coefficient of DPP (0.1 $\mu m^2\ s^{-1}$, measured by photobleaching and recovery[32]) is low enough to be consistent with thermal diffusion, its movement within and between epithelial cells is thought to be active and to require endocytosis (however, an alternative hypothesis does exist[33]). Thus, unlike the case of the RanGTP gradient, the DPP gradient is thought to rely on active diffusion. By contrast, a gradient of the morphogen fibroblast growth factor in the zebrafish embryo, the length constant of which is ≈200 μm, is established by rapid thermal diffusion through the extracellular space (D ≈100 $\mu m^2\ s^{-1}$, measured by fluorescence correlation spectroscopy) and exocytosis-dependent removal in the tissue[34]. These examples show that the gradients of morphogens in tissues can vary considerably in length scale, which in these cases is determined primarily by variation in the diffusion coefficients. Interestingly, in these examples, the active diffusion is slower than thermal diffusion; perhaps active processes allow tighter control of morphogen spread.

Surprisingly, the mechanism underlying the BCD protein gradient in the *D. melanogaster* embryo is not settled, despite BCD being the first morphogen to be discovered[4]. Local source–global sink models[35,36] have proposed that BCD diffuses away from its site of synthesis at the anterior pole (the local source, in this case *bcd* mRNA) and is degraded throughout the tissue (the global sink). However, photobleaching and recovery experiments indicate a very small diffusion coefficient of 0.3 $\mu m^2\ s^{-1}$; this is too low to explain a BCD gradient with a characteristic length of ≈100 μm. This is because the diffusion time ($\lambda^2/(2D)$ = 16,000 s) is longer than the time that it takes to establish the protein gradient *in vivo* (5,000 s)[37]. An alternative to a reaction–diffusion mechanism is that BCD is nearly immobile and remains near to where it is synthesized, leading to a protein localization that reflects *bcd* mRNA gradient[38]. However, a large diffusion coefficient of 7 $\mu m^2\ s^{-1}$ has been measured by fluorescence correlation spectroscopy[39]; this is high enough to explain the formation of a BCD protein gradient by a reaction–diffusion mechanism. This example illustrates both the difficulty of doing quantitative measurements in developing tissues and the importance of these measurements in understanding patterning mechanisms.

Patterns generated by a Turing mechanism. Historically, a 'Turing pattern' refers to a time-invariant pattern with a well-defined wavelength (length scale) produced by a reaction–diffusion system containing two or more chemical species with distinct diffusion coefficients. Turing patterns (FIG. 1d,e) have been used to model regeneration in hydra[1,2], the patterns on seashells[40] and the striped pigmentation in fish[41] (FIG. 1f). In the case of zebrafish, there is good evidence for short-range activation and long-range inhibition, which are the requirements for a Turing pattern; however, the identities of the activator and inhibitor are not known. In other systems, candidate inhibitor and activator molecules have been identified, but whether a Turing mechanism is responsible for generating the pattern is not clear[5]. To prove that a Turing mechanism underlies pattern formation, it will be important to measure rates of diffusion and reaction and show that they can

quantitatively account for the spatial period and dynamics of the patterns.

Patterns generated by advection and diffusion. When advection moves material in one direction and diffusion tends to move the material in the opposite direction (down its concentration gradient), a new length scale emerges: $\lambda = D/v$ (FIG. 2a). An example of this is the localization of myosin motor proteins at the tips of the stereocilia of hair cells (FIG. 2b), which is thought to be due to the combination of directed movement of the motor along the actin filaments within the stereocilia (advection) and diffusion that occurs when the motor detaches from the actin[42]. The stereocilia form the hair bundle, the mechanosensitive organelle of these cells, and proper stereocilial length, which is essential for hearing, is regulated by myosins[43], although how exactly the motor localization controls length is still not understood.

Antenna mechanism. A particularly interesting example of length determination takes place when the reaction involves the shortening of the polymer track on which active transport is occurring[44,45]. In this example, kinase-interacting protein 3 (Kip3) motors (which belong to the Kinesin-8 family) bind randomly along the length of a microtubule at a rate r_{on} per unit length of microtubule (proportional to the cytoplasmic Kip3 concentration); they move processively to the end of the microtubule and then remove a tubulin dimer before dissociating (FIG. 2c). This gives a depolymerization rate that depends on the microtubule length: the longer the microtubule, the more motors land on it, the greater the flux of motors to the end and therefore the higher the rate of depolymerization. Thus, the microtubule acts as an antenna for motors. If the microtubule polymerization rate in the absence of motors (r_+, which is proportional to the bulk tubulin concentration) is independent of length, and if the motor speed is much faster than the rate of microtubule growth due to polymerization, the characteristic length is $\lambda = r_+/r_{on}$ (REF. 46) (FIG. 2d), which increases with the tubulin concentration and decreases with the motor concentration. The length is independent of the motor velocity, and only requires that the motors be fast enough to outpace growth and processive enough to reach the microtubule end.

This mechanism accounts for the role of Kinesin-8 in controlling the overall length of the mitotic spindle, as well as its role in centring the chromosomes in the metaphase spindle, which requires that the two half spindles (which span between the poles and the chromosomes) be the same length[47–49]. In this mechanism, the motor proteins act as molecular rulers that pace out the lengths of the microtubules; they then use depolymerization as a readout of the length.

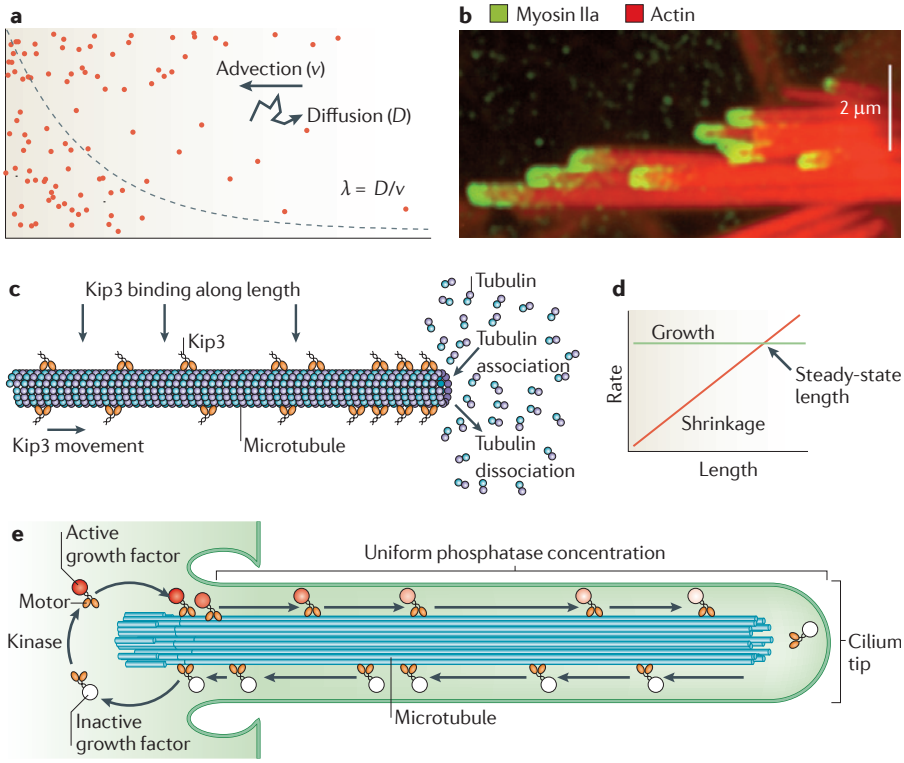

Figure 2 | **Patterning by motor-mediated transport. a** | Schematic of patterning by advection and diffusion. Molecules (red dots) are actively transported to the left, whereas diffusion tends to make them move to the right. This establishes a gradient with a length scale $\lambda = D/v$, in which D is the diffusion coefficient and v is the speed of advective transport. **b** | The advection of myosin IIa towards the tips of the stereocilia of hair cells is driven by myosin's intrinsic motor activity[57]. **c** | Schematic of the antenna mechanism for microtubule length control. Kinase-interacting protein 3 (Kip3) motors (which belong to the Kinesin-8 family) bind to a microtubule with a rate r_{on} per microtubule length. The motors then move to the microtubule's plus end and depolymerize it by removing tubulin subunits. If the motor speed greatly exceeds the microtubule's growth rate in the absence of Kip3 (r_+) then the length of the microtubule will be equal to r_+/r_{on}. **d** | The microtubule reaches its steady-state length when the growth and shrinkage rates are equal[46]. **e** | Schematic of an advection–reaction model, a hypothetical mechanism for the length control of cilia and microvilli. Cargoes, for example growth factors, carried along cilia and microvilli are inactivated over time by phosphatases, which may provide a length-dependent signal to the growing tip. Image in part **d** is modified, with permission, from REF. 46 © (2007) Elsevier.

Patterns formed by advection and reaction. Patterns can also be generated by a combination of advection and reaction: the length scale is $\lambda = v/k$. Although no biological lengths are known to be regulated by such a mechanism, there are numerous candidates. For example, if motor proteins carry cargo molecules along the cytoskeletal filaments within cilia and microvilli, and the cargoes are inactivated over time, for example by phosphatases, then the deactivation of the cargoes could provide a length-dependent signal to the growing tip of the cilium or microvillus (FIG. 2e).

Patterns generated by viscosity and friction. Active material properties can also define length scales. Consider a viscoelastic material, such as a contractile tissue or the thin actomyosin cortex located under the plasma membrane of a cell. A gradient of motor activity in the material will create an active stress gradient and lead to a velocity gradient; over long timescales, the material behaves as a viscous fluid. If there is friction with the surroundings, for example between the tissue and an adjacent rigid extracellular matrix or between the

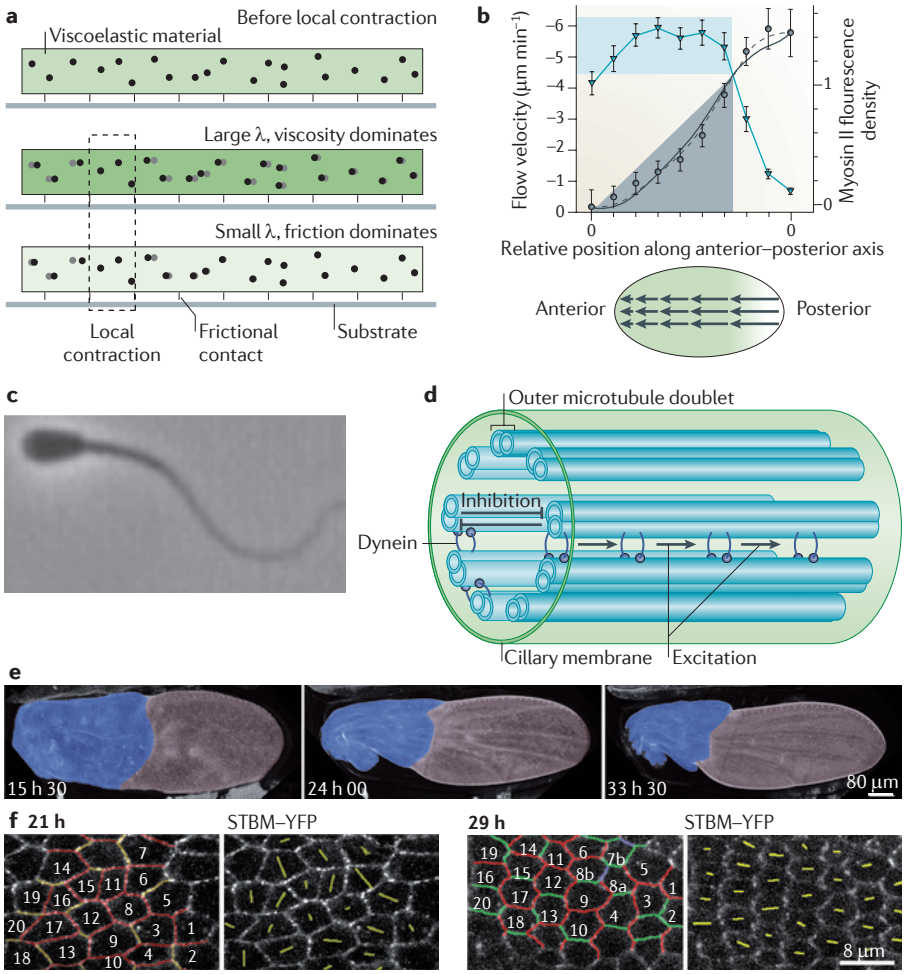

Figure 3 | **Length scales set up by stresses. a** | A viscoelastic tissue makes frictional contact with an adjacent surface; tracer particles (black dots) embedded in it allow one to track the motion (upper panel). A local region of high contractile stress leads to flow (represented as movement of the tracer particles, shown in grey), the velocity of which decays with a length $\lambda = \sqrt{(\eta/\gamma)}$, in which η is the viscosity and γ is the friction coefficient. When λ is large, the flow pattern decays gradually (middle panel); when λ is small, the flow pattern decays quickly (lower panel). **b** | Contractility gradients drive flow over a characteristic length. The graph (top panel) shows the distribution of contractility as determined by measuring myosin concentration (blue) and the resulting flow velocity profile (grey) plotted against position along the *Caenorhabditis elegans* zygote (bottom panel; in which arrows indicate flow). Note that there are significant flows (shaded grey) in regions where contractility is relatively constant (shaded blue), indicative of long-range flow. Fitting reveals that the characteristic length $\lambda = \sqrt{(\eta/\gamma)}$ is roughly 30% of the embryo size. **c**,**d** | A snapshot of a freely swimming bull sperm (**c**). The length is 60 μm from head to tail. The movement of the sperm flagellum is controlled by a mechanical signalling pathway. This regulates the reciprocal activity of the dynein motors across the section of the axoneme (the inner cytoskeletal structure comprising microtubules) and coordinates the wave of activity that travels from head to tail[26] (**d**). **e**,**f** | Strabismus (STBM; a *Drosophila melanogaster* protein involved in planar cell polarity during wing development) tagged with yellow fluorescent protein (YFP) at various times after puparium formation. The contraction of the hinge (blue) changes the shape of the wing blade (**e**) and leads to a reorganization and reorientation of the wing epithelial cells (**f**). Colour coding of cell boundaries: yellow, disappear; red, persist; green, resulting from neighbour exchange. Yellow bars indicate ordering of planar cell polarity. Images in part **b** are modified, with permission, from REF. 23 © (2010) Macmillan Publishers Ltd. All rights reserved. Images in parts **e** and **f** are reproduced, with permission, from REF. 55 © (2010) Elsevier.

cortex and the cell wall, then the velocity gradient will have the characteristic length $\lambda = \sqrt{(\eta/\gamma)}$, in which η is the viscosity and γ is the friction coefficient[50,51] (FIG. 3a).

This mechanism has been proposed to operate in polarizing long-range cortical flow in the *Caenorhabditis elegans* embryo[23] (FIG. 3b). Contraction of the anterior cortex induces anterior-directed cortical flows, which in turn transport polarity and cell-fate determining proteins into the anterior half of the cell. Importantly, if contraction causes flows that carry regulators of contraction, such as partitioning defective (PAR) proteins[52,53], then the feedback can lead to mechanochemical pattern formation[51] (BOX 1).

From pattern to shape

Patterning is often taken to refer to the spatial distribution of biochemical species. In this paper, we have defined patterning in a more general sense, namely any feature of a length scale far beyond that of molecular size. In this sense, patterning also refers to the generation of shapes, allowing for a more complete description of morphology. The formation of shape is an inherently mechanical process that requires deformation of the biological material. In contrast to reaction–diffusion mechanisms, which are only capable of biochemical patterning, mechanical processes can both pattern and shape concurrently, as Turing proposed at the beginning of his paper.

A beautiful example of shaping is the serpentine beating of cilia and flagella, for example in sperm (FIG. 3c). Mechanical force associated with microtubule sliding is thought to coordinate dynein motor activity[26] (FIG. 3d), which in turn generates the bending forces that create the beating pattern, the wavelength of which is typically between 10 μm and 100 μm and the frequency of which is typically between 10 Hz and 100 Hz (REF. 54). The wave speed is therefore between 100 μm s^{-1} and 10,000 μm s^{-1}, and diffusion would be much too slow to coordinate the beating.

Another example in which long-range mechanical forces play crucial parts in patterning is the developing fly wing (FIG. 3e,f). Contraction at the wing base orients the elongation, division and packing of the wing epithelial cells, causing both an elongation of the wing and a realignment of the axis of planar polarity of the cells with the long axis of the developing wing[55]. These two examples demonstrate that mechanical signals can be faster and more long-range than chemical signals that are transported by thermal diffusion alone.

Summary

We have described several examples in which active mechanical processes, driven by forces generated by motor proteins, pattern and shape cells and tissues. The key idea behind patterning is that there must be signalling over distances comparable to the features in the pattern. Turing explored the

Box 1 | **Biochemical and mechanical coupling**

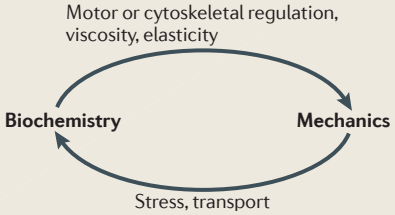

The interdependence of biochemical and mechanical processes is a central theme in morphogenesis. These processes sometimes operate independently or in parallel, but most often they involve networks of feedback loops among the constitutive components, both biochemical and mechanical in nature (see the figure). For example, biochemical regulation of cytoskeletal mechanics through actin or tubulin polymerization and motor protein activity has a marked effect on cellular or tissue mechanics. At the same time, unevenly distributed mechanical stresses result in material movement, which advectively transports the very components regulating the mechanics. This can result in a local build-up of the biochemical regulators of stress, creating a positive feedback loop. As Alan Turing noted[1], morphogens may also affect osmotic pressure and electrical and viscoelastic material properties, adding another level of mechanical and biochemical coupling. Furthermore, stresses can also realign the cytoskeletal filaments[56], thereby altering the delivery of chemical signals by motor proteins. Such complex networks of mechanics and chemistry, marked by feedback loops, are commonplace in developmental processes, underscoring the need to consider coupled chemical and mechanical processes in the study of morphogenesis.

case in which diffusion of chemical species carries the signal. We have discussed how directed transport and mechanical forces generated by motor proteins can also transmit signals over space to create patterns. Other mechanisms are no doubt possible.

In addition to biochemical patterning, mechanical processes can also shape cells and tissues. We believe that cell and tissue mechanics will be crucial to understanding many of the outstanding questions in morphology, such as how gastrulation works and how organs are shaped and sized. The mechanochemical approach is a natural extension of the ideas that Turing suggested but left unfinished owing to his untimely death.

Jonathon Howard and Stephan W. Grill are at the Max Planck Institute of Molecular Cell Biology and Genetics, Pfotenhauerstr. 108, 01307 Dresden, Germany.

Stephan W. Grill is also at the Max Planck Institute for the Physics of Complex Systems, Nöthnitzer Str. 38, 01187 Dresden, Germany.

Justin S. Bois is at the Department of Chemistry and Biochemistry, University of California, Los Angeles, California 90095, USA.

e-mails: howard@mpi-cbg.de; grill@mpi-cbg.de; justinbois@gmail.com

doi:10.1038/nrm3120

1. Turing, A. M. The chemical basis of morphogenesis. *Proc. R. Soc. Lond. B Biol. Sci.* **237**, 37–72 (1952).
2. Gierer, A. & Meinhardt, H. A theory of biological pattern formation. *Kybernetik* **12**, 30–39 (1972).
3. Wolpert, L. Positional information and the spatial pattern of cellular differentiation. *J. Theor. Biol.* **25**, 1–47 (1969).
4. Frohnhöfer, H. N. C. & Nüsslein-Volhard, C. Organization of the anterior pattern in the *Drosophila* embryo by the maternal gene *bicoid*. *Nature* **324**, 120–125 (1986).
5. Kondo, S. & Miura, T. Reaction-diffusion model as a framework for understanding biological pattern formation. *Science* **329**, 1616–1620 (2010).
6. Huxley, A. F. & Niedergerke, R. Structural changes in muscle during contraction. Interference microscopy of living cells. *Nature* **173**, 971–976 (1954).
7. Huxley, H. E. & Hanson, J. Changes in the cross-striations of muscle during contraction and stretch and their structural interpretion. *Nature* **173**, 973–976 (1954).
8. Gibbons, I. R. & Rowe, A. J. Dynein: a protein with adenosine triphosphatase activity from cilia. *Science* **149**, 424–426 (1965).
9. Brady, S. T. A novel brain ATPase with properties expected for the fast axonal transport motor. *Nature* **317**, 73–75 (1985).
10. Vale, R. D., Reese, T. S. & Sheetz, M. P. Identification of a novel force-generating protein, kinesin, involved in microtubule-based motility. *Cell* **42**, 39–50 (1985).
11. Crick, F. Diffusion in embryogenesis. *Nature* **225**, 420–422 (1970).
12. Howard, J. *Mechanics of Motor Proteins and the Cytoskeleton* (Sinauer Associates, Sunderland, Massachusetts, 2001).
13. Luby-Phelps, K. Cytoarchitecture and physical properties of cytoplasm: volume, viscosity, diffusion, intracellular surface area. *Int. Rev. Cytol.* **192**, 189–221 (2000).
14. Helenius, J., Brouhard, G., Kalaidzidis, Y., Diez, S. & Howard, J. The depolymerizing kinesin MCAK uses lattice diffusion to rapidly target microtubule ends. *Nature* **441**, 115–119 (2006).
15. Gutzeit, H. O. & Koppa, R. Time-lapse film analysis of cytoplasmic streaming during late oogenesis of *Drosophila*. *J. Embryol. Exp. Morphol.* **67**, 101–111 (1982).
16. Goldstein, R. E., Tuval, I. & van de Meent, J.-W. Microfluidics of cytoplasmic streaming and its implications for intracellular transport. *Proc. Natl Acad. Sci. USA* **105**, 3663–3667 (2008).
17. Short, M. B. *et al.* Flows driven by flagella of multicellular organisms enhance long-range molecular transport. *Proc. Natl Acad. Sci. USA* **103**, 8315–8319 (2006).
18. Baas, P. W., Deitch, J. S., Black, M. M. & Banker, G. A. Polarity orientation of microtubules in hippocampal neurons: uniformity in the axon and nonuniformity in the dendrite. *Proc. Natl Acad. Sci. USA* **85**, 8335–8339 (1988).
19. Snider, J. *et al.* Intracellular actin-based transport: how far you go depends on how often you switch. *Proc. Natl Acad. Sci. USA* **101**, 13204–13209 (2004).
20. Zimyanin, V. L. *et al. In vivo* imaging of *oskar* mRNA transport reveals the mechanism of posterior localization. *Cell* **134**, 843–853 (2008).
21. Wilhelm, C. Out-of-equilibrium microrheology inside living cells. *Phys. Rev. Lett.* **101**, 028101 (2008).
22. Engler, A. J., Sen, S., Sweeney, H. L. & Discher, D. E. Matrix elasticity directs stem cell lineage specification. *Cell* **126**, 677–689 (2006).
23. Mayer, M., Depken, M., Bois, J. S., Jülicher, F. & Grill, S. W. Anisotropies in cortical tension reveal the physical basis of polarizing cortical flows. *Nature* **467**, 617–621 (2010).
24. Rauzi, M., Lenne, P.-F. & Lecuit, T. Planar polarized actomyosin contractile flows control epithelial junction remodelling. *Nature* **468**, 1110–1114 (2010).
25. Zerzour, R., Kroeger, J. & Geitmann, A. Polar growth in pollen tubes is associated with spatially confined dynamic changes in cell mechanical properties. *Dev. Biol.* **334**, 437–446 (2009).
26. Howard, J. Mechanical signaling in networks of motor and cytoskeletal proteins. *Annu. Rev. Biophys.* **38**, 217–234 (2009).
27. Vogel, V. & Sheetz, M. Local force and geometry sensing regulate cell functions. *Nature Rev. Mol. Cell Biol.* **7**, 265–275 (2006).
28. Brown, G. C. & Kholodenko, B. N. Spatial gradients of cellular phospho-proteins. *FEBS Lett.* **457**, 452–454 (1999).
29. Wartlick, O., Kicheva, A. & González-Gaitán, M. Morphogen gradient formation. *Cold Spring Harb. Perspect. Biol.* **1**, a001255 (2009).
30. Kalab, P., Weis, K. & Heald, R. Visualization of a Ran-GTP gradient in interphase and mitotic *Xenopus* egg extracts. *Science* **295**, 2452–2456 (2002).
31. Caudron, M., Bunt, G., Bastiaens, P. & Karsenti, E. Spatial coordination of spindle assembly by chromosome-mediated signaling gradients. *Science* **309**, 1373–1376 (2005).
32. Kicheva, A. *et al.* Kinetics of morphogen gradient formation. *Science* **315**, 521–525 (2007).
33. Belenkaya, T. Y. *et al. Drosophila* Dpp morphogen movement is independent of dynamin-mediated endocytosis but regulated by the glypican members of heparan sulfate proteoglycans. *Cell* **119**, 231–244 (2004).
34. Yu, S. R. *et al.* Fgf8 morphogen gradient forms by a source-sink mechanism with freely diffusing molecules. *Nature* **461**, 533–536 (2009).
35. Driever, W. & Nüsslein-Volhard, C. A gradient of *bicoid* protein in *Drosophila* embryos. *Cell* **54**, 83–93 (1988).
36. Gregor, T., Bialek, W., de Ruyter van Steveninck, R. R., Tank, D. W. & Wieschaus, E. F. Diffusion and scaling during early embryonic pattern formation. *Proc. Natl Acad. Sci. USA* **102**, 18403–18407 (2005).
37. Gregor, T., Wieschaus, E. F., McGregor, A. P., Bialek, W. & Tank, D. W. Stability and nuclear dynamics of the bicoid morphogen gradient. *Cell* **130**, 141–152 (2007).
38. Spirov, A. *et al.* Formation of the bicoid morphogen gradient: an mRNA gradient dictates the protein gradient. *Development* **136**, 605–614 (2009).
39. Abu-Arish, A., Porcher, A., Czerwonka, A., Dostatni, N. & Fradin, C. High mobility of Bicoid captured by fluorescence correlation spectroscopy: implication for the rapid establishment of its gradient. *Biophys. J.* **99**, L33–L35 (2010).
40. Meinhardt, H. *The Algorithmic Beauty of Sea Shells* (Springer, Berlin; London, 2009).
41. Nakamasu, A., Takahashi, G., Kanbe, A. & Kondo, S. Interactions between zebrafish pigment cells responsible for the generation of Turing patterns. *Proc. Natl Acad. Sci. USA* **106**, 8429–8434 (2009).
42. Naoz, M., Manor, U., Sakaguchi, H., Kachar, B. & Gov, N. S. Protein localization by actin treadmilling and molecular motors regulates stereocilia shape and treadmilling rate. *Biophys. J.* **95**, 5706–5718 (2008).
43. Manor, U. *et al.* Regulation of stereocilia length by myosin XVa and whirlin depends on the actin-regulatory protein Eps8. *Curr. Biol.* **21**, 167–172 (2011).
44. Varga, V. *et al.* Yeast Kinesin-8 depolymerizes microtubules in a length-dependent manner. *Nature Cell Biol.* **8**, 957–962 (2006).
45. Varga, V., Leduc, C., Bormuth, V., Diez, S. & Howard, J. Kinesin-8 motors act cooperatively to mediate length-dependent microtubule depolymerization. *Cell* **138**, 1174–1183 (2009).
46. Howard, J. & Hyman, A. A. Microtubule polymerases and depolymerases. *Curr. Opin. Cell Biol.* **19**, 31–35 (2007).
47. Mayr, M. *et al.* The human kinesin Kif18A is a motile microtubule depolymerase essential for chromosome congression. *Curr. Biol.* **17**, 488–498 (2007).
48. Stumpff, J., Vondassow, G., Wagenbach, M., Asbury, C. & Wordeman, L. The Kinesin-8 motor Kif18A suppresses kinetochore movements to control mitotic chromosome alignment. *Dev. Cell* **14**, 252–262 (2008).
49. Wargacki, M. M., Tay, J. C., Muller, E. G., Asbury, C. L. & Davis, T. N. Kip3, the yeast Kinesin-8, is required for clustering of kinetochores at metaphase. *Cell Cycle* **9**, 2581–2588 (2010).

50. Salbreux, G., Prost, J. & Joanny, J.-F. Hydrodynamics of cellular cortical flows and the formation of contractile rings. *Phys. Rev. Lett.* **103**, 058102 (2009).
51. Bois, J., Jülicher, F. & Grill, S. Pattern formation in active fluids. *Phys. Rev. Lett.* **106**, 028103 (2011).
52. Munro, E., Nance, J. & Priess, J. R. Cortical flows powered by asymmetrical contraction transport PAR proteins to establish and maintain anterior-posterior polarity in the early *C. elegans* embryo. *Dev. Cell* **7**, 413–424 (2004).
53. David, D. J. V., Tishkina, A. & Harris, T. J. C. The PAR complex regulates pulsed actomyosin contractions during amnioserosa apical constriction in *Drosophila*. *Development* **137**, 1645–1655 (2010).
54. Riedel-Kruse, I. H., Hilfinger, A., Howard, J. & Jülicher, F. How molecular motors shape the flagellar beat. *HFSP J.* **1**, 192 (2007).
55. Aigouy, B. *et al.* Cell flow reorients the axis of planar polarity in the wing epithelium of *Drosophila*. *Cell* **142**, 773–786 (2010).
56. Hamant, O. *et al.* Developmental patterning by mechanical signals in *Arabidopsis*. *Science* **322**, 1650–1655 (2008).
57. Schneider, M. E., Dosé, A. C., Salles, F. T., Chang, W. *et al.* A new compartment at stereocilia tips defined by spatial and temporal patterns of myosin IIIa expression. *J. Neurosci.* **26**, 10243–10252 (2006).

Acknowledgements
We thank N. Goehring, M. Mayer and F. Jülicher for discussions, and I. Tolic-Norrelykke for comments on the manuscript.

Competing interests statement
The authors declare no competing financial interests.

FURTHER INFORMATION
Jonathon Howard's homepage: http://www.mpi-cbg.de/nc/research/research-groups/joe-howard
Stephan W. Grill's homepage: http://www.mpi-cbg.de/research/research-groups/stephan-grill.html
Justin S. Bois's homepage: http://www.justinbois.info
ALL LINKS ARE ACTIVE IN THE ONLINE PDF